Memoryless AM/AM Behavioral Model for RF Power Amplifiers

Paul O. Fisher[1,2] and Said F. Al-Sarawi[1]

[1]School of Electrical and Electronic Engineering, The University of Adelaide, SA 5005, Australia
Email: (paul.fisher@adelaide.edu.au; said.alsarawi@adelaide.edu.au)
[2]RF Industries, (RFI), Allenby Gardens, SA, 5009, Australia
Email: (paul.fisher@rfi.com.au)

Abstract— This paper presents a technique that allows a simple semi-physical amplitude-modulation-to-amplitude-modulation (AM/AM) model for RF power amplifier modeling, over a wide range of solid state technologies, with improved accuracy. The proposed technique builds on a recent memoryless behavioral model (BM), recently proposed by Cann, and demonstrates between 5 dB to 20 dB normalized mean squared error (NMSE) improvement, compared to the existing memoryless BM model, in AM/AM modeling over a range of RF power amplifier (RF PA) technologies, through comparison with our and other measured data from the literature. In addition, it provides an accurate prediction of third order intermodulation distortion (3rd IMD) linearization improvement of up to 17 dB. The proposed model can be used for system modeling or RF PA linearization applications. Issues related to segmentation discontinuities are also discussed.

Index Terms—Memoryless Behavioral Models, Simulation, Linearizer, Low Cost, RF Power Amplifiers, Analog Predistortion, Adjacent Channel.

I. INTRODUCTION

With the ever pressing demands for modern wireless communications systems to provide increased data capacity, as well as reduced spectral emissions and increased power efficiencies, RF PA devices play a crucial role in being able to achieve these demanding goals. As such improved behavioral modeling of PA devices at the system level is essential. Having a simple, fast and efficient BM that can be used over a range of device technologies, for RF PA devices, would be most advantageous in allowing the RF PA designer the ability to select this RF PA device quickly and accurately from a range of different devices and technologies.

Recent approaches for providing linear communication systems are to utilize advanced digital processing techniques which can be complex, expensive and less power efficient. However, in applications where the emphasis is more on simple, low cost and efficient solutions rather high performance, e.g. Small Cell repeaters [1], there is a need to develop techniques that allow for improved modeling accuracy while considering device operation over a wider dynamic range. This can have added benefits for use with envelope-tracking, predistortion linearizers that operate over larger dynamic ranges [2].

A new quasi memoryless (QM) BM for amplitude-modulation-to-phase-modulation (AM/PM) was recently described by Glock *et al.* [3]. The rationale for the development of this model is that simple static models are both less complex

and less computationally intensive. Their work emphasized that memory effects are less prominent in well designed RF PAs and thus can be reduced to an acceptable level for mobile handset applications by careful amplifier biasing [4]. Their model addresses certain phase responses in semiconductor technologies such as gallium arsenide (GaAs) and Complementary Metal Oxide Semiconductor (CMOS).

Solid State device AM/AM responses are of the same generic shape, hence having a semi-physical model to estimate the AM/AM response of these devices with improved accuracy over a large dynamic range and range of technologies would be beneficial. Such models are of significant advantage to RF PA designers as they allow system modeling and performance evaluation without the need for complex and in depth device models.

This paper only focuses on AM/AM modeling, and does not cover AM/PM modeling in investigating how simple modeling can be used to quickly asses RF PA device performance for solid state devices, as AM/PM performance can be considered to be small enough to be neglected [5]. This will also reduce the complexity and computation times thus aiding in a faster device selection process. Improving the AM/AM modeling accuracy will also benefit the RF PA device selection process. Section II presents the need for simple BMs, including a brief review of other modeling approaches and technology modeling capabilities. Section II-D presents a new method that is based on a recent AM/AM model which is capable of producing the correct 3rd IMD response in the small signal region. Benefits of BM accuracy improvements to linearizer performance are discussed in Section III. A segmentation and optimization method is proposed and discussed in Section IV further improving the overall accuracy of the AM/AM model and demonstrating its applicability over a range of different technologies. Consideration of the proposed model and accuracy improvement method, with respect to 3rd IMD performance and impact on linearization improvement are discussed in Section V. Followed by a conclusion and acknowledgment.

A summary of the contributions presented in this paper are: (i) an optimized segmented curve-fitting approach, using a recent improved accuracy AM/AM model, providing up to 20 dB NMSE improvement, (ii) demonstrated improvement of up to 17 dB in linearizer 3rd IMD predication, (iii) an accurate AM/AM model that is applicable for a wide range of solid

IEEE computer society

state power amplifier technologies, (iv) a model parameter fitting approach that uses a simple algorithm and simulation that takes into account segment boundary discontinuities, and (v) demonstrating that worst case discontinuities have no noticeable effect on the modeled amplifier spectrum when using digitally modulated signals.

II. SSPA Behavioral Models

A. The Need for Simple Models

One of the major factors contributing to the performance degradation of a wireless system are the non-linearities contributed by RF PAs, so for a system level evaluation the impact of this amplifier on the system's performance needs to be investigated. This can be achieved using detailed RF PA device parameters and accurate nonlinear models. However for an initial system level evaluation such information may not be available or may require too much effort to obtain. In addition, such modeling is computationally intensive and requires very long simulation times. In contrast, a system level modeling that use simple bandpass BMs of an RF PA can result in fast, but still accurate, simulations that can be used to assess the RF PA technologies and their impact on system performance. Hence allowing for rapid RF PA device comparisons, evaluations and selections.

The envelope model describing an RF PAs non-linearities, in terms of its AM/AM and AM/PM responses, can be derived from the complex input to output envelope voltage relationship as given by

$$v_{out}(t) = \mathrm{Re}\left[G(v(t))e^{j(\phi(t)+\varphi(v(t))+\omega_c t)}\right], \tag{1}$$

where ω_c is the RF carrier frequency, $G(v(t))$ and $\varphi(v(t))$ describe the instantaneous input to output envelope voltage gain and phase and these represent the RF PA's AM/AM and AM/PM responses, respectively. Some of these can be obtained from the manufacturer's datasheet or through further measurements and testing.

As part of performing a rapid and accurate system analysis, and selecting the RF PA device, then having a semi-physical based device BM provides the very significant benefit of the best starting point for least squared curve fitting (LSCF) that will typically be required in order to extract these model's parameters, plus any non-physical model parameters. This is extremely important and powerful for practical PA designers as it provides them with a fast way of assessing suitable PA device alternatives, using parameters that are readily available in device datasheets, without the need for further complex testing and measurements. Only the smoothness parameter, s, is non-physical. By having a unified physical or semi-physical AM/AM model that spans a range of solid state power amplifier technologies, is simple and computationally efficient, then this will greatly facilitate system level modeling.

B. Review of Simple PA Behavioral Models

In the literature several well established memoryless BMs offer PA designers with both a simple and fast means to conduct system level modeling, hence allowing them to be used for selecting a suitable device to meet system level requirements. Of these BMs, Cann 1980 [6] introduced a semi-physical AM/AM memoryless model. The model can be used for an over driven or soft-limiting bipolar based solid state amplifier by allowing the knee sharpness to be adjusted. Then Saleh [7] introduced a simple behavioral model that requires only 2 parameters for both AM/AM and AM/PM modeling, however this model was focused around Traveling Wave Tube Amplifiers (TWTAs). Another model that specifically targeted modeling the AM/AM and AM/PM of SSPAs was proposed by Ghorbani and Sheikhan [8]. Both the AM/AM and AM/PM models have the same form, and use only 4 parameters, while addressing inaccuracies associated with using TWTA based models for SSPAs. It is worth mentioning that the parameters for these models were not physically based.

At the same time Rapp [5], presented another memoryless AM/AM model for GaAs FET SSPAs that did included semi-physical parameters. Later on Honkanen and Haggman [9] applied Rapp's model as part of a bipolar junction transistor (BJT) AM/AM model. They also provided a new AM/PM model however it has the limitation of a maximum zero degrees phase shift. Then new models for AM/AM and AM/PM where introduced by White *et al.* [10] to better model Ka Band SSPAs. The proposed model for Ka band SSPAs provided improved accuracy when compared to the Saleh, Ghorbani and Rapp models.

Saleh's model was further developed by O'Droma *et al.* [11], with respect to Laterally Diffused Metal Oxide Semiconductor (LDMOS) field-effect-transistors (FETs), addressing the discontinuity seen in the application of Saleh's original AM/PM model when applied to typical LDMOS AM/PM characteristics, thus making Saleh's TWTA model suitable for use with solid state devices, however the parameters are still not physically based.

Cann 2012 [12] updated his earlier model to eliminate issues found with the original model when calculating small signal 3rd order IMD products, with the model again based on semi-physical parameters.

Recently Glock [3] presented an approach based around Rapp's AM/AM model but introduced a new AM/PM model determined from the first derivative of the Rapp AM/AM model plus additional terms.

The O'Droma model [11], can provide an excellent fit to a range of AM/AM and AM/PM curve shapes but the parameters for this model do not have a physical origin. As a result, determining the starting point values for this and other non-physically based model parameters for LSCF can be difficult and may require more sophisticated methods to determine these starting point values. So an appropriate selection of the starting points is needed to ensure an optimum outcome. With semi-physical based models, the majority of parameter starting points are taken from available data, thus avoiding possible guessing or further measurements.

For the non-physical parameters of the Rapp and recent Cann 2012 AM/AM only models, several plots of the AM/AM

responses can be made for a particular device, for different s values. By comparing these plots with measured data, an estimate of the starting value for s can be found. Having semi-physical starting points is also a very useful means of self checking the LSCF parameter results, as the final values for LSCF parameter results should be very close to the starting values.

C. Comparing PA Behavioral Models

To facilitate comparing these BMs, the NMSE in dB can be used. The definition that will be used through out this paper is given by [13]

$$\text{NMSE}_{\text{dB}} = 10 \log_{10} \left(\frac{\sum_{n=0}^{N} |y_{MOD}[n] - y[n]|^2}{\sum_{n=0}^{N} |y[n]|^2} \right), \quad (2)$$

where N is the number of samples, $y[n]$ is the complex baseband envelope of the measured PA output and $y_{MOD}[n]$ is the complex baseband envelope of the model output.

To evaluate these BMs and new method in the frequency domain, comparisons are made using Simulink, where a wide-band code division multiple access (WCDMA) baseband envelope digitally modulated signal is applied to the RF PA model and the output is presented in the frequency domain via the Simulink Fast Fourier Transform (FFT) based spectrum analyzer element, for the AM/AM models described in this paper.

D. AM/AM Model Selection

Rapp's AM/AM model [5], used by Glock, has the same equation form as the model originally proposed by Cann but without the modulus function. Cann's original 1980 AM/AM model equation is given as

$$A(r) = \frac{L \text{sgn}(r)}{\left[1 + \left(\frac{L}{g|r|}\right)^s\right]^{1/s}} = \frac{gr}{\left[1 + \left(\frac{g|r|}{L}\right)^s\right]^{1/s}}, \quad (3)$$

where g, r, L and s are the small signal gain, input amplitude, output limit level, and sharpness parameters, respectively.

Litva and Lo [14] identified that Cann's original 1980 AM/AM model had issues related to correctly generating 3rd IMD responses in the small signal region. This was confirmed and the reason for this issue was determined by Loyka [15]. Cann's new memoryless 2012 AM/AM model, presented recently, is given as [12]

$$A(r) = \frac{L}{s} \ln \left[\frac{1 + e^{s(\frac{gr}{L}+1)}}{1 + e^{s(\frac{gr}{L}-1)}} \right] - L, \quad (4)$$

where g, r, L and s are the small signal gain, input amplitude, output limit level, and sharpness parameters, respectively. It should be noted that the issues in the old model are related to modeling two discrete tones used to generate IMD products, however for a typical digital modulation scheme no issues were observed. This improved AM/AM model will be used as the basis for our modeling method.

III. LINEARIZER BENEFITS FROM ACCURACY IMPROVEMENTS

For simple low cost RF predistortion linearizers to be able to compete with more sophisticated linearizers, like DPD linearizers having complex and expensive hardware with higher power consumption, then the accuracy of low cost RF predistortion linearizers must be comparable to DPD linearizers [1]. To quantify the benefits of AM/AM modeling accuracy improvement, when applied to a low cost RF predistortion linearizer, a means of quantifying this benefit is required. Based on an analysis by Nojima and Konno [16], an equation for calculating the amount of 3rd IMD reduction, S_{IMD}, achievable from a predistorter (PD) and power amplifier as function of the AM/AM and AM/PM errors, is given by

$$S_{IMD} = -10 \log_{10} \left[1 + 10^{\delta A/10} - 2 \cdot 10^{\delta A/20} \cos(\delta\theta) \right], \quad (5)$$

where δA and $\delta\theta$ are the amplitude error in dB and the phase error in degrees respectively. For this combination, the amount of distortion reduction achievable is a function of the amplitude and phase errors as contributed by the PD. If the PD errors are considered to be fixed, then any degradation in the intermodulation distortion reduction can be attributed to BM amplitude inaccuracies for a fixed phase. The impact of AM/AM modeling improvement on the IMDs and linearization performance, due to this model is discussed further in Section V.

IV. SEGMENTED CURVE FITTING METHOD TO IMPROVE AM/AM MODEL ACCURACY

Similar to the techniques utilized by Glock to determine the linear, non-linear and saturation regions from the AM/AM characteristic response, this technique can also be utilized to determine the linear, non-linear or saturation region segments of the AM/AM responses of Cann's 2012 AM/AM model. Furthermore, the curve fits of these segments can be applied in a similar approach to that used by Zhu *et al*, [2], for piecewise curve fitting of non-linear segments of AM/AM and AM/PM envelop-tracking amplifiers. As a result, the segmented curve fitting provides more accurate model results and assists with comparing devices for system analysis purposes, as well as defining potential improvements in linearization margin for a particular device.

By applying the recent Cann 2012 AM/AM model for each segmented region across a range of technologies and by optimizing the end of the linear region segment and start of the saturation region segment, an overall improvement of between 5 dB to 20 dB can be achieved in AM/AM NMSE at the expense of further simple processing steps for each segment, depending on RF PA device technology. The recent Cann 2012 AM/AM model also has the ability to provide starting values for LSC fitting for each of the segments.

To improve the AM/AM accuracy estimation of this model, the second derivative of the AM/AM response is used to determine both the linear and saturation regions. Using AM/AM data from Glock's Fig. 11 2V2 curve, it can be seen that

more data points are required when penetrating further into the saturation region, so the approach developed by [17], based on Rapp's AM/AM model, to extrapolate the AM/AM performance into the saturation region can be used. As Glock's paper uses the Rapp AM/AM model then this AM/AM data can be extended into the saturation region. Similarly for Cann's recent 2012 AM/AM model, data can be extended into the saturation region. Using the extended AM/AM data, the transition from the linear to saturation regions can be determined as a function of v_{in} when the 2nd derivative of the AM/AM data equals zero, see Fig. 1. As can be seen from this plot, the linear region stop point (vertical blue solid line) is at $v_{in} = 0$ V and saturation region start point (vertical orange solid line) is well beyond the available data, by the 2nd derivative calculation. This means that the practical LSCF data starting range extends from $v_{in} = 0$ V to where v_{in} is at the full extent of the available data (vertical red solid line), in this case where $v_{in} = 0.5$ V. The region between the solid blue and red lines is practically the full AM/AM model region for initial LSCF with these points being the starting points for the AM/AM segmentation method optimization.
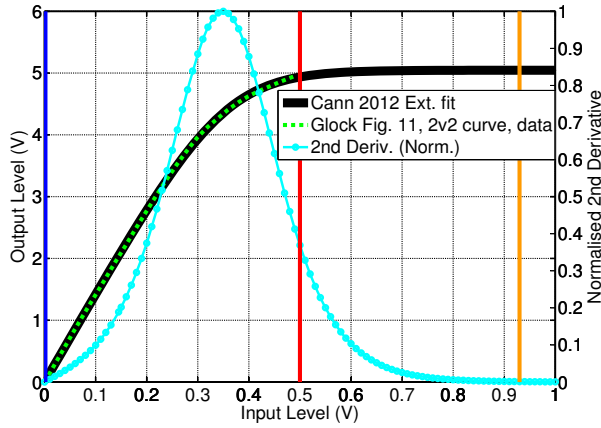

Fig. 1. Glock's Fig. 11, 2V2 curve, [3] AM/AM data (green dotted curve), extended AM/AM data (solid black curve), using [17] & normalised (to the maximum value) numerical 2nd derivative of extended AM/AM data (cyan solid circle curve) using Matlab. The solid blue vertical line is the initial end of the linear region, the solid orange vertical line is start of saturation region by the 2nd derivative calculation. The solid red vertical line is the end of the available AM/AM data, effectively the end of the saturation region for the available data.

Initial AM/AM curve fits for both the recent Cann 2012 and Glock (using Rapp's AM/AM model) AM/AM models have been performed over the entire available data for Glock's Fig. 11, 2V2 curve data, with the results from both the Glock (using Rapp's AM/AM model) (green down triangle curve) and the recent Cann 2012 AM/AM (magenta circle curve) models shown in Fig. 2. These are single segment fits between the linear region stop and saturation region start points. This is the same as using the AM/AM model over the entire available data range.
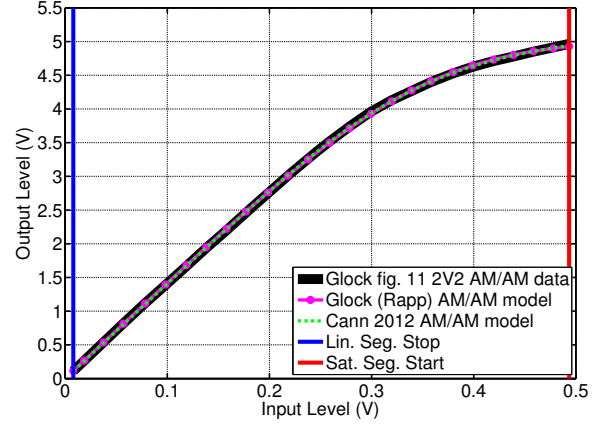

Fig. 2. Comparison of curve fit for Glock's Fig. 11, 2V2 curve, data [3] (black solid curve), Glock's (using Rapp's AM/AM model) AM/AM model (green dotted curve) & recent Cann 2012 AM/AM model (magenta solid circle trace).

A. Optimized Segmented Curve Fitting

To further improve the accuracy of the AM/AM model an optimization routine was developed to identify the optimum linear stop and saturation start region points to provide an enhanced data fit in terms of NMSE performance. A comparison between the initial fit and the optimised fit for each of the segments is shown in Fig. 3 (yellow curves). This is only shown for the recent Cann 2012 AM/AM model.
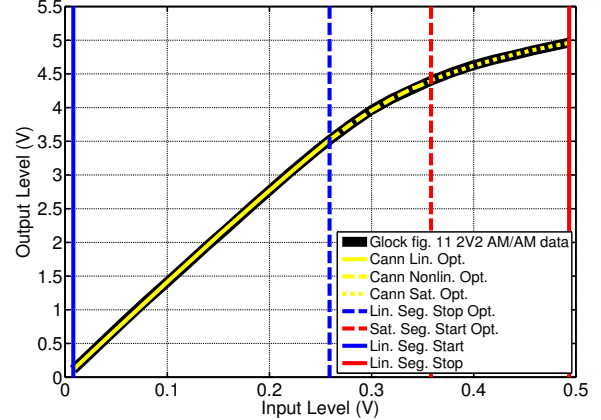

Fig. 3. Comparison of curve fit for Glock's Fig. 11, 2V2 curve, data [3] (black solid curve) and the optimised segmented curve fits for the recent Cann 2012 AM/AM model (yellow curves). The optimised linear segment is between the input voltage range of 0 V to 0.26 V, with the optimised non-linear segment between 0.26 V and 0.36 V and the remaining saturation segment is between 0.36 V and 0.5 V.

When comparing the LSC fit over the full range of data, Fig. 2, compared to the segmented linear, non-linear and saturation region data, Fig. 3, it is difficult to see any difference. However a comparison between the Glock (using Rapp's AM/AM model) and recent Cann 2012 absolute AM/AM errors (in dB), for both initial and optimised segmentation versus input voltage for Glock's Fig. 11, 2V2 curve, data are shown in

Fig. 4, reveals the improvements in absolute error obtained by using the segmentation method. The improvements can be seen between the Cann 2012 (solid magenta) and segmented Cann 2012 (solid red) curves. The initial maximum error result is shown as the horizontal dotted magenta line with the optimised segmented result shown as the horizontal red dash - dot line. An NMSE AM/AM comparison between these models and the corresponding improvements using the segmentation technique show, following segmentation optimization, that the recent Cann 2012 AM/AM model has better than 10 dB improvement. In Section V, Table I shows the improvements in NMSE by using the segmentation method over a range of technologies.
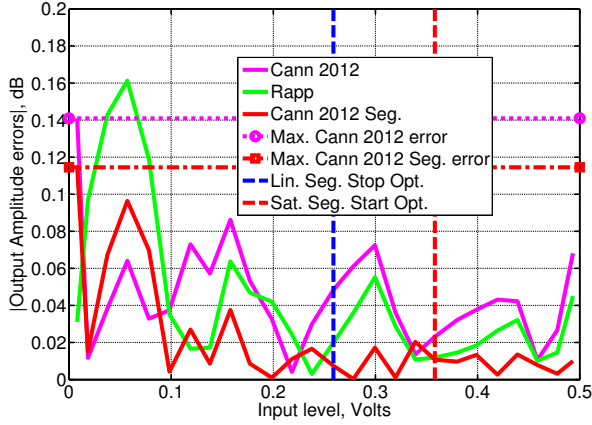

Fig. 4. Comparison of |Output Amplitude errors| versus input voltage from Glock's Fig. 11, 2V2 curve, data [3], showing before and after segmented approach optimization. Also shown are the maximum for Cann's recent 2012 AM/AM model amplitude errors for both the initial (magenta solid line) & segmented (red solid line) approach being 0.14 and 0.115 dB respectively.

An algorithm for optimising segmented curve fitting was prepared to further improve NMSE and is presented as Algorithm 1. The algorithm starting points for the second derivatives cannot be zero due to their numerical nature, so there is a requirement to have 2nd derivative zero limits, in our case we have selected this value to be below 0.001, to suit the numerical data. During the minimisation process there are some segment ranges where the discontinuities are higher than the given data resulting in poorer segment fits. This is due to using parameter starting values for the full range of data in those segments. This can be corrected by determining suitable starting points for each segment but this has not been implemented within this algorithm. Even with such improvement in the starting point, the overall curve fit performance is still worse than the segmented approach.

B. Frequency Domain Comparisons & Discontinuity Effects at Segment Boundaries

A comparison of the recent Cann 2012 model, with and without optimised segmentation, against measured data with a WCDMA signal applied, for the SHF-0189 HFET [18] are given in Fig. 5. These plots show that the optimized segmented

---

Algorithm 1 Minimize AM/AM NMSE in dB

Require: Combined AM/AM NMSE (dB) linear, non-linear & saturation region segments are minimum.

Ensure: V_{in} & V_{out} are real & > 0.

1: **INPUT** V_{out} vs. V_{in} data-set for the amplifier.
2: Determine $d''V_{out}/dV_{in}$ (2nd Derivative)
3: **if** $d''V_{out}/dV_{in} \neq 0$ after the first occurrence when $d''V_{out}/dV_{in} = 0$ **then**
4:    V_{out} vs. V_{in} data does not extend far enough into the saturation region so extend the V_{out} vs. V_{in} data using [17], refer to Fig.1.
5: **end if**
6: **if** $d''V_{out}/dV_{in} = 0$, on the first occurrence. **then**
7:    $V_{in_{Lin}}$ is the linear region *stop* point.
8: **else if** $d''V_{out}/dV_{in} = 0$, on the second occurrence. **then**
9:    $V_{in_{Sat}}$ is the saturation region *start* point.
10: **end if**
11: Note: V_{out} vs. V_{in} data between $V_{in_{Lin}}$ & $V_{in_{Sat}}$ is the non-linear region data.
12: **for** $V_{in} = 0$ to $V_{in_{Lin}}$ **do**
13:    Least Squares Curve Fit (LSCF) V_{out} vs. $V_{in_{Lin}}$ using (4)
14: **end for**
15: **for** $V_{in} = V_{in_{Lin}}$ to $V_{in_{Sat}}$ **do**
16:    LSCF V_{out} using (4), for the non-linear region.
17: **end for**
18: **for** $V_{in} = V_{in_{Sat}}$ to $V_{in_{max}}$ **do**
19:    LSCF V_{out} vs. $V_{in_{Sat}}$ using (4), for the saturation region data.
20: **end for**
21: **for** $V_{in} = 0$ to $V_{in_{max}}$ **do**
22:    Calculate AM/AM NMSE A (dB), using (2), for the combined linear, non-linear & saturation region segments.
23:    Adjust $V_{in_{Lin}}$ & $V_{in_{Sat}}$ to give $V_{in_{Lin1}}$ & $V_{in_{Sat1}}$
24: **end for**
25: **repeat**
26:    Steps 12: to 24: using $V_{in_{Lin1}}$ & $V_{in_{Sat1}}$ calculate AM/AM NMSE B (dB), using (2), for the *combined* linear, non-linear & saturation region segments.
27: **until** NMSE B (dB) < NMSE A (dB)
28: Note: It may occur that NMSE A (dB) < NMSE B (dB), i.e. the initial segmentation is optimum.
29: Output all calculated curve fit coefficients. **END**

---

method provides a better fit to the measured data compared to the non segmented model.

To determine the effects of discontinuities at segment boundaries, investigations have revealed that although the recent Cann 2012 AM/AM model, using the optimised segmentation method does not have continuous derivatives over the segment boundaries, the voltage errors between the segment boundaries, after optimization, are very small and have a negligible effect on the adjacent channel leakage ratio (ALCR) response. This has been investigated for a WCDMA digitally
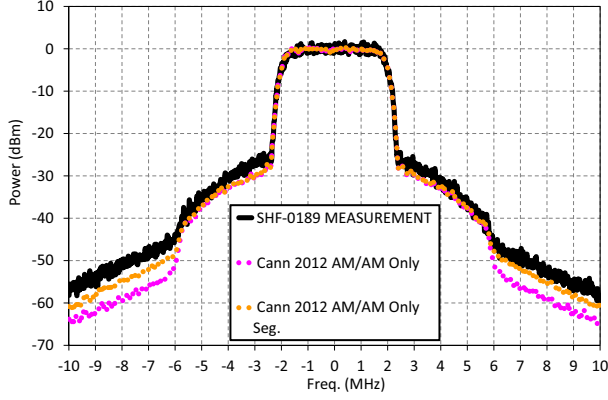
Fig. 5. Comparison of measured versus Simulink simulations for WCDMA, comparing Glock versus recent Cann 2012 full & optimized segmented models for the SHF-0189, [18], data. Resolution bandwidth (RBW) for both measured & simulation data is 30 kHz. Measured center frequency is 881.5 MHz.

modulated signal with the same power spectral density level as used in Glock's Fig. 9. The worst case discontinuity error, of 0.0111 volts, for either of the linear to nonlinear or nonlinear to saturation segment boundaries was increased, above the optimised value, until the second ACLR level increased by ≈ 1 dB and this occurred at 10 times the worst case discontinuity error with no noticeable increase found for the first ACLR, concluding that the optimized segmented recent Cann 2012 AM/AM model has negligible discontinuity effects, even when considering worst case discontinuities at the segment boundaries. Comparisons between the optimized segmentation discontinuity error result and 10 times this error are shown in Fig. 6.

V. IMPACT ON IMDs & LINEARIZATION IMPROVEMENT

Cann's recent 2012 AM/AM model and the optimised segmentation method have been assessed to determine how they perform in predicting 3rd IMD performance for RF PAs over a wide dynamic range by simulating the 3rd IMDs using Simulink and comparing the simulations against manufacturer's measured IMD data, SHF-0189 device [19] page 5. Plots of the 3rd IMD comparisons are shown in Fig. 7 with comparisons of the absolute 3rd IMD errors shown in Fig. 8. The results indicate that the recent Cann 2012 AM/AM model performs better than the Rapp or O'Droma (Modified Saleh) AM/AM models, even though the O'Droma (Modified Saleh) model shows very good curve fitting results. The recent Cann 2012 AM/AM model has ≈ 2.6 dB improvement in average error (AE) compared to the O'Droma model and over 10 dB AE improvement compared to the Glock (using Rapp's AM/AM model) model. The optimized segmented recent Cann model method improves the AE by a further ≈ 0.7 dB.

The maximum absolute amplitude error, of the full and optimised segmented recent Cann 2012 AM/AM model of Glock's Fig. 11 AM/AM device data from LSC fitting, are 0.141 dB and 0.115 dB respectively. These are shown on a plot of (5),
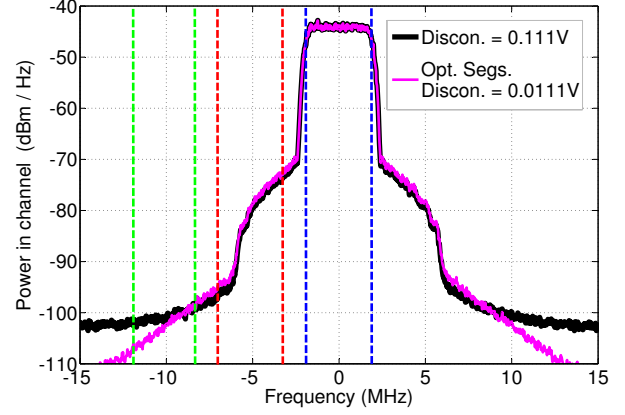

Fig. 6. Discontinuity effects on a WCDMA modulated signal, simulated using Simulink, for Cann's recent 2012 optimized segmented AM/AM model of Glock's Fig.11, 2V2 curve, data [3] data. With 0.0111 volt discontinuity ACLR1L/2L = -33.2/-57.3 dBc. With 0.111 volt discontinuity ACLR1L/2L = -33.7/-56.2 dBc. In-band wanted between dashed blue vertical lines, ACLR1 between dashed red vertical lines and ACLR2 between dashed green vertical lines (lower bands only shown) with 3.84 MHz integration bandwidth (BW). The integrated power over the wanted 3.84 MHz BW is 21.6 dBm. RBW is 30 kHz.
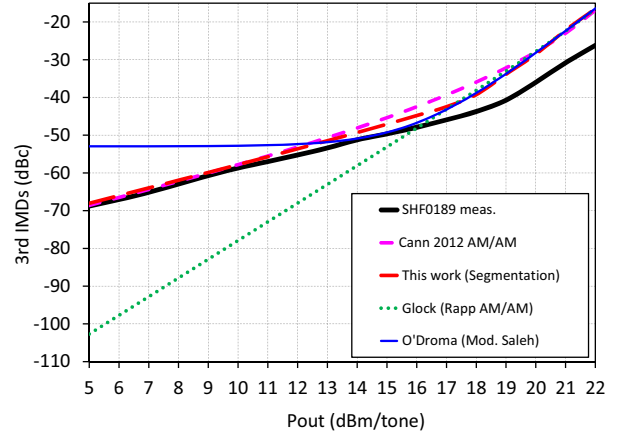

Fig. 7. 3rd IMD measured device data SHF-0189 [19] page 5 versus Simulink simulated comparison of the O'Droma (Mod. Saleh), Glock & recent Cann 2012 models, all including both AM/AM components. Two tone measurements at 900 MHz, 1 MHz tone spacing.

Fig. 9, where the intermodulation distortion improvement is plotted against phase error for various amplitude errors. The difference between the full and optimised segmented method equates to a 3rd IMD improvement of 1.79 dB at 0.1° phase error.

Table I shows the NMSE for each of the various technologies, BJT, heterojunction FET (HFET), LDMOS FET, heterojunction-bipolar-transistor (HBT), enhancement mode pseudomorphic high-electronmobility-transistor (E-pHEMT), GaAs (Glock's Fig. 8 device data), CMOS (Glock's Fig. 11 device data) and galliun nitride (GaN) on silicon carbide
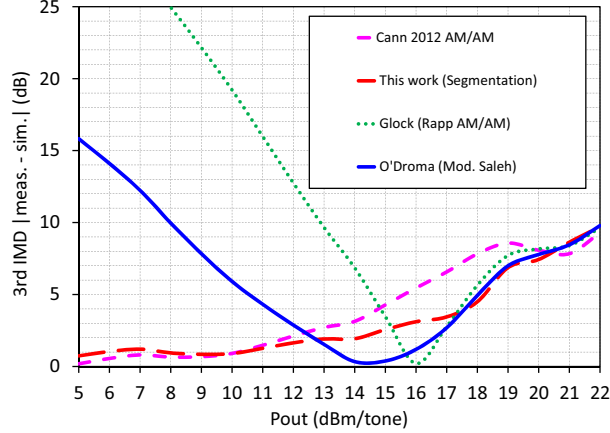
Fig. 8. 3rd IMD |measured minus Simulink simulated| error for the O'Droma (Mod. Saleh), Glock (using Rapp's AM/AM model), recent Cann 2012 & optimized segmented recent Cann 2012 models for AM/AM only. The AE for Cann's recent 2012 AM/AM model is $\approx$ 4dB compared to $\approx$ 6.5 & 13.9 dB for the O'Droma and Glock (using Rapp's AM/AM model) models respectively. The optimized segmented recent Cann 2012 model AE further improves 3rd IMD over the recent Cann 2012 model by $\approx$ 0.7 dB.

(GaN/SiC) HEMT. The AM/AM NMSEs were determined for both the full and segmented methods. Table I also shows the 3rd IMD linearization improvement across device technology as a result of the optimised segmentation method AM/AM improvements.
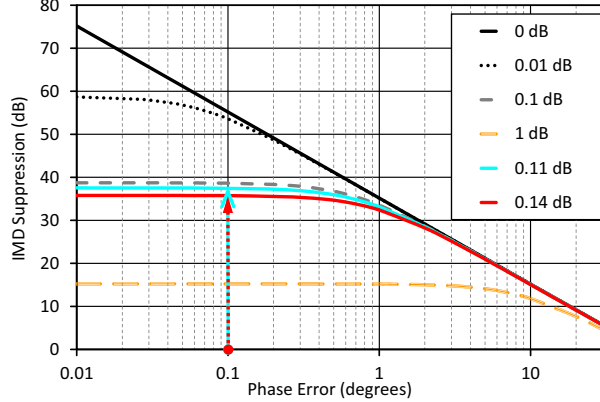

Fig. 9. IMD suppression versus phase errors for a range of amplitude errors. The cyan vertical arrow shows the 3rd IMD improvement in linearization for the optimised segemnted approach compared to the full recent Cann 2012 AM/AM model, red dotted vertical arrow, both at $0.1°$ phase error.

VI. CONCLUSION

In this paper we have presented and demonstrated the use of a more accurate simple AM/AM model that is suitable for use over a range of RF PA device technologies.

A segmented curve-fitting approach, using the proposed recent AM/AM model, has also been presented that provides up to 20 dB Normalized Mean Squared Error (NMSE) improvement when modeling the AM/AM characteristics of the

TABLE I
TECHNOLOGY NMSE & LINEARIZATION IMPROVEMENT COMPARISON

Device [Ref.]	Cann 12B AM/AM NMSE (dB)		NMSE Imp. (dB)	IMD Imp. (dB)
	Full	Seg.		
BJT [9]	-30.16	-35.28	5.12	3.02
HFET [18]	-43.53	-62.84	19.31	13.51
HBT [20]	-58.88	-64.86	5.98	6.43
E-pHEMT [21]	-44.77	-63.41	18.64	13.90
LDMOS [22]	-37.68	-42.40	4.72	1.39
GaAs [3]	-39.61	-58.20	18.59	0.75
CMOS [3]	-46.04	-56.07	10.03	1.79
GaN/SiC [23]	-43.10	-48.40	5.30	17.62

amplifier, further resulting in linearizer 3rd IMD improvements of up to 17 dB.

A model parameter fitting approach using a simple algorithm has been indicated along with simulations accounting for segment boundary discontinuities, demonstrating that such worst case discontinuities have no effect on the modeled amplifier spectrum when using digitally modulated signals.

Future work will be to investigate improving AM/PM modeling accuracy and to combine that work with this current work on AM/AM modeling to determine how the combined AM/AM and AM/PM accuracy improvements will increase linearizer 3rd IMD performance.

REFERENCES

[1] J. Xia, A. Islam, H. Huang, and S. Boumaiza, "Envelope memory polynomial reformulation for hardware optimization of analog-RF predistortion," *IEEE Microwave and Wireless Components Letters*, vol. 25, no. 6, pp. 415–417, June 2015.

[2] A. Zhu, P. J. Draxler, C. Hsia, T. J. Brazil, D. F. Kimball, and P. M. Asbeck, "Digital predistortion for envelope-tracking power amplifiers using decomposed piecewise Volterra series," *IEEE Transactions on Microwave Theory and Techniques*, vol. 56, no. 10, pp. 2237–2247, Oct 2008.

[3] S. Glock, J. Rascher, B. Sogl, T. Ussmueller, J.-E. Mueller, and R. Weigel, "A memoryless semi-physical power amplifier behavioral model based on the correlation between AM-AM and AM-PM distortions," *IEEE Transactions on Microwave Theory and Techniques*, vol. 63, no. 6, pp. 1826–1835, June 2015.

[4] Y. S. Lee, M. W. Lee, S. H. Kam, and Y. H. Jeong, "A high-linearity wideband power amplifier with cascaded third-order analog predistorters," *IEEE Microwave and Wireless Components Letters*, vol. 20, no. 2, pp. 112–114, Feb 2010.

[5] C. Rapp, "Effects of HPA-nonlinearity on a 4-DPSK/OFDM-signal for a digital sound broadcasting signal," in *Proceedings Second European Conf. on Sat. Comm. (ESA SP-332), Liege, Belgium*, oct 1991, pp. 179–184.

[6] A. Cann, "Nonlinearity model with variable knee sharpness," *IEEE Transactions on Aerospace and Electronic Systems*, vol. AES-16, no. 6, pp. 874–877, 1980.

[7] A. Saleh, "Frequency-independent and frequency-dependent nonlinear models of TWT amplifiers," *IEEE Transactions on Communications*, vol. 29, no. 11, pp. 1715–1720, 1981.

[8] A. Ghorbani and M. Sheikhan, "The effect of solid state power amplifiers (SSPAs) nonlinearities on MPSK and M-QAM signal transmission," in *Sixth International Conference on Digital Processing of Signals in Communications*, Sep 1991, pp. 193–197.

[9] M. Honkanen and S.-G. Haggman, "New aspects on nonlinear power amplifier modeling in radio communication system simulations," in *IEEE International Symposium on Personal, Indoor and Mobile Radio Communications, PIMRC*, vol. 3, 1997, pp. 844–848.

[10] G. White, A. Burr, and T. Javornik, "Modelling of nonlinear distortion in broadband fixed wireless access systems," *Electronics Letters*, vol. 39, no. 8, pp. 686–687, 2003.

[11] M. O'Droma, S. Meza, and Y. Lei, "New modified Saleh models for memoryless nonlinear power amplifier behavioural modelling," *IEEE Communications Letters*, vol. 13, no. 6, pp. 399–401, 2009.

[12] A. Cann, "Improved nonlinearity model with variable knee sharpness," *IEEE Transactions on Aerospace and Electronic Systems*, vol. 48, no. 4, pp. 3637–3646, 2012.

[13] M. Isaksson, D. Wisell, and D. Ronnow, "A comparative analysis of behavioral models for RF power amplifiers," *IEEE Transactions on Microwave Theory and Techniques*, vol. 54, no. 1, pp. 348–359, 2006.

[14] J. Litva and T. K.-Y. Lo, Eds., *Digital Beamforming in Wireless Communications*, 1st ed. Norwood, MA, USA: Artech House, Inc., 1996, ch. 4, sec. 4.4.1, pp. 79-81.

[15] S. Loyka, "On the use of Cann's model for nonlinear behavioral-level simulation," *IEEE Transactions on Vehicular Technology*, vol. 49, no. 5, pp. 1982–1985, 2000.

[16] T. Nojima and T. Konno, "Cuber predistortion linearizer for relay equipment in 800 MHz band land mobile telephone system," *IEEE Transactions on Vehicular Technology*, vol. 34, no. 4, pp. 169–177, Nov 1985.

[17] P. Fisher and S. Al-Sarawi, "Improving the accuracy of SSPA device behavioral modeling," in *International Conference on Information and Communication Technology Research, ICTRC*, 2015, pp. 278–281.

[18] Sirenza Microdevices. (EDS-101240 Rev E) SHF-0189, 0.05 - 6 GHz, 0.5 Watt GaAs HFET. [Online]. Available: http://datasheet.octopart. com/SHF-0189-Sirenza-datasheet-129519.pdf

[19] ——. (EAN-101798 Rev A) SHF-0189, Amplifier Application Circuits, DESIGN APPLICATION NOTE — AN-031. [Online]. Available: http://application-notes.digchip.com/147/147-47818.pdf

[20] NXP. (Revision: 9, October, 2014) MMG3005NT1, 800 - 2000 MHz, Heterojunction Bipolar Transistor. [Online]. Available: http://nxp.com/

[21] Avago Technologies. (February 10, 2014) ALM-31122, 700 MHz - 1 GHz E-pHEMT, 1 Watt High Linearity Amplifier. [Online]. Available: http://www.avagotech.com/

[22] Ampleon. (Revision: 4 - 1 September, 2015) BLM7G1822S-20, 1805 MHz to 2170 MHz, LDMOS 2-stage power MMIC. [Online]. Available: http://www.ampleon.com/

[23] Northrop Grumman. (Revision: May, 2014) APN180, 27-31 GHz GaN Power Amplifier. [Online]. Available: http://www.northropgrumman. com/